

Molecular weight dependence of reductions in the glass transition temperature of thin, freely standing polymer films

K. Dalnoki-Veress,^{1,2} J. A. Forrest,³ C. Murray,¹ C. Gigault,¹ and J. R. Dutcher¹

¹*Department of Physics and the Guelph-Waterloo Physics Institute, University of Guelph, Guelph, Ontario, Canada N1G 2W1*

²*Department of Physics and Astronomy, McMaster University, Hamilton, Ontario, Canada L8S 4M1*

³*Department of Physics, University of Waterloo, Waterloo, Ontario, Canada N2L 3G1*

(Received 19 January 2000; revised manuscript received 10 July 2000; published 20 February 2001)

We have used transmission ellipsometry to perform a comprehensive study of the glass transition temperature T_g of freely standing polystyrene films. Six molecular weights \bar{M}_w , ranging from 575×10^3 to 9100×10^3 , were used in the study. For each \bar{M}_w value, large reductions in T_g (as much as 80°C below the bulk value) were observed as the film thickness h was decreased. We have studied in detail the dependence of the T_g reductions on \bar{M}_w in a regime dominated by chain confinement effects. The empirical analysis presented is highly suggestive of the existence of a mechanism of mobility in thin freely standing films that is inhibited in the bulk and distinct from the usual cooperative motion associated with the glass transition.

DOI: 10.1103/PhysRevE.63.031801

PACS number(s): 36.20.-r, 64.70.Pf, 68.60.Bs, 65.40.De

INTRODUCTION

Despite considerable experimental and theoretical efforts, the nature of the glass transition remains unresolved. Theoretical attempts to describe the glass transition include phenomenological ones such as free volume descriptions [1], treatment as a real thermodynamic phase transition [2], and purely kinetic ones [3]. While many theoretical descriptions are able to provide some insight into the glass transition, there are no definitive treatments. One concept that is becoming increasingly recognized as fundamental to descriptions of the glass transition dynamics is that of cooperative motion. The idea, which was first introduced empirically by Adam and Gibbs [4], is that for sufficiently supercooled liquids structural relaxation may take place only if a number of the constituent particles rearrange collectively. This cooperativity may be used to describe a length scale encompassing the cooperative region, which increases in size as the temperature is lowered. Recent simulations of supercooled glass forming liquids have shown the existence of stringlike cooperative motion, with a length scale increasing as the temperature is lowered [5]. The existence of a length scale for cooperative motion suggests the possibility of *finite size effects*; changes in the glass transition temperature and dynamics when the system is confined to systems near the cooperativity size. In the kinetic glass transition the structural properties of the melt and the glass are not distinguishable and the existence of finite size effects is perhaps the only way first to ascertain the existence of and then to quantify a characteristic length scale for glass transition dynamics.

The search for finite size effects in glass forming systems has involved confinement in porous glass [6,7], layered silicates [8], entangled polymers [9], and thin films [10]. The first systematic studies of the glass transition in confined geometries involved using calorimetric techniques to measure the glass transition temperature T_g of glass forming organic liquids confined to the pores of controlled pore glass [6]. These studies revealed a T_g value that was reduced below the bulk value for the confined liquids, the maximum T_g

reduction being 18°C for *o*-terphenyl confined to 4 nm pores. More recent studies have employed dielectric loss measurements to examine relaxation in similar confined liquids [7] and have revealed faster dynamics consistent with the lower T_g values reported. These studies have been explained as being a natural result of the length scale of cooperative dynamics. For the case where the molecules at the boundary have enhanced mobility, once the cooperativity size becomes greater than the sample size, fewer molecules are involved in rearrangements in the confined system than in the equivalent bulk system and the confined system has faster dynamics. The majority of studies on confined glass formers have concentrated on samples that are small molecule liquids confined to pore glass. While it is obvious that such samples do allow for essentially bulk quantities of highly confined samples to be prepared and measured, there are reasons why such samples are not necessarily the best for these studies. Even for pores treated with special chemicals to promote ‘‘lubrication’’ at the surfaces, there is no straightforward way to confirm the surface chemistry. Furthermore, the studies are necessarily restricted to employing confining dimensions and pore size distributions that are available to pore glasses.

Thin polymer films are an ideal sample geometry in the search for finite size effects. The confining dimension, the film thickness, is easily varied from nanometers to micrometers and the interaction with the substrate is easily controlled and readily quantified. There have been many studies of the glass transition in thin polymer films in recent years, motivated by the original, extensive ellipsometry study by Keddie *et al.* of thin polystyrene (PS) films on Si substrates [11,12]. In that study, the authors observed reduced values of T_g with decreasing film thickness h for $h \leq 40$ nm, with no strong dependence of the results on the molecular weight of the PS molecules. It is worth emphasizing that in *all* studies of T_g in thin films of PS, the *measured* T_g values were observed to be reduced below the bulk value for sufficiently thin films. Additional studies [13–16] have revealed that the expansivities of the glass and melt phases of thin polymer films may be different from the bulk values. This has been shown to lead to difficulties in identifying the T_g values [10]. Despite an

apparent controversy between results of Refs. [11,12,14–20] and that of Ref. [13], it is a fact that there are no reports of *measured* T_g values for PS films that actually increase as the film thickness is decreased [21]. Measurements of chain diffusion that appear to contradict this statement of consensus between experiments should not be compared directly with T_g values because it is only the *temperature dependence* of the diffusion constant that is related to T_g , and this has yet to be measured. While for the case of PS the experimental consensus is overwhelming in the qualitative observation of a reduced T_g for thin films, there is scatter in the actual measured values between different groups which may be attributed to different strengths of interaction between the polymer and substrates. More definitive work on the effect of this interfacial interaction on the T_g value has involved the use of different polymers. For thin films of poly(methyl methacrylate) the measured T_g value could be either greater than or less than the bulk value depending on the substrate [12], and by using different polymer tacticities a direct relation was found between the density of polymer-substrate interactions and the effect on the T_g value [22].

Freely standing polymer films provide an ideal sample geometry for two reasons. First, the sample geometry is simplified because it is symmetric with respect to the midplane of the film, instead of the asymmetric geometry of supported films. Secondly, and of considerable importance, the interpretation of the T_g results for freely standing films is not complicated by the presence of an interaction with an underlying substrate. In Brillouin light scattering (BLS) measurements of T_g in freely standing PS films [17,18], reductions in T_g with decreasing h as large as 70 °C were measured, which are much larger than those measured for supported PS films of the same thickness. Also, in measurements of $T_g(h)$ in freely standing PS films with two different values of the molecular weight \bar{M}_w [18], a large dependence of the T_g reduction on \bar{M}_w was measured. This is qualitatively different from the results obtained for supported PS films. This early study suggested that the dependence of the T_g reductions on \bar{M}_w is a clear indication that *chain confinement* effects are important, but since it involved only two values of \bar{M}_w it was not enough to quantify the effect. In addition, this large change in the dynamics due to confinement of the polymer chain occurs for film thicknesses for which there appear to be no coincident changes in the structure [23]. In any case it is clear that a detailed and quantitative study of the \bar{M}_w dependence of the T_g value in thin freely standing films of PS is needed. While a recent study has shown that for much smaller values of \bar{M}_w the \bar{M}_w dependence vanishes [14,19], this does not help to elucidate the origin of the chain confinement effects. For a detailed review of the literature on the glass transition in confined geometries, we refer the reader to [10,24].

The purpose of the present article is to provide a study of the \bar{M}_w dependence of the T_g reductions with sufficient detail to allow a complete analysis. This quantification is required to achieve a deeper understanding of chain confinement effects on T_g in freely standing polymer films. We have

TABLE I. Molecular weight \bar{M}_w , polydispersity index \bar{M}_w/\bar{M}_n , and root-mean-square end-to-end distance R_{ee} of the PS used in the present study. Also listed are the best fit values of the slope α and threshold thickness h_0 obtained by fitting Eq. (2) to the data shown in Fig. 4.

\bar{M}_w	\bar{M}_w/\bar{M}_n	R_{ee} (nm)	α (°C/nm)	h_0 (nm)
575 000	1.12	56	1.48 ± 0.13	67.7 ± 0.7
767 000	1.11	64	1.68 ± 0.13	70.8 ± 0.7
1 250 000	1.06	82	2.02 ± 0.13	76.9 ± 0.7
2 240 000	1.08	110	2.41 ± 0.13	80.4 ± 0.7
6 680 000	1.22	190	3.21 ± 0.13	86.5 ± 0.7
9 100 000	1.22	222	3.36 ± 0.13	87.8 ± 0.7

used the technique of transmission ellipsometry to obtain very precise measurements of $T_g(h)$ for six different \bar{M}_w values. While the results of the present study do not allow an unambiguous identification of the mechanism responsible for the T_g reductions in thin polymer films, the reliable and reproducible nature of the data will allow stringent tests of theories of the effect of chain confinement on T_g in thin polymer films.

EXPERIMENT

Sample preparation

Narrow distribution polystyrene with six molecular weights ranging from $\bar{M}_w = 575 \times 10^3$ to 9100×10^3 was obtained from Polymer Source Inc. The molecular weight, polydispersity index, and root-mean-square end-to-end distance of the molecules are listed in Table I. Thin PS films were prepared on carefully cleaned glass substrates or freshly cleaved mica substrates by spin-coating solutions of PS dissolved in toluene. Solutions with PS mass concentrations of 0.6% to 1.5% were spin coated at speeds of 1500 to 5000 rpm to obtain the film thicknesses used in this study.

After spin coating, the PS films on the substrates were annealed in vacuum at 115 °C for 12 h. The annealing procedure serves both to remove any solvent that may be trapped in the films and to relax the chains after the spin-coating procedure. The samples were then cooled to room temperature at a rate of 1 °C/min. A water transfer technique [18] was used to place the PS film across a 4 mm diameter hole in sample holders made of either stainless steel or nylon (polyamide 66), creating a freely standing film. For the present study, more than 40 different freely standing PS films were prepared and measured.

Measurement of the glass transition temperature

Previous ellipsometric studies of T_g in thin polymer films have involved films supported by substrates, and have thus necessarily used the technique of reflection ellipsometry [11,12,18]. For optically transparent samples such as the polystyrene freely standing films used in this study, transmission ellipsometry may be used. For this case the lack of substrate offers a simpler analysis. In transmission mode

nulling ellipsometry experiments, circularly polarized laser light is passed through a polarizer, through a quarter-wave plate, and transmitted through a thin film sample. The polarizer is rotated such that the light transmitted through the sample is linearly polarized. The transmitted light is then extinguished by a cross-polarized analyzer placed before an optical detector [25]. For an isotropic transparent film, measurement of the rotation angles of the polarizer (P) and the analyzer (A) corresponding to a null in the intensity at the detector can be used to obtain values of the film thickness h and the index of refraction n at the laser wavelength, using standard ellipsometry equations [25].

A custom-built, single-wavelength, self-nulling ellipsometer was used to measure the glass transition temperature T_g of freely standing PS films. The careful design of the ellipsometer allowed us to measure the P and A angles with high precision, typically $\pm 0.002^\circ$. Initially, we performed both reflection and transmission ellipsometry measurements on the freely standing PS films. However, because of sample vibrations, transmission ellipsometry was found to produce more reliable and less noisy results.

The ellipsometry measurements at different temperatures T were performed by placing the sample in an optical furnace which also allowed modest cooling below room temperature ($-5^\circ\text{C} < T < 120^\circ\text{C}$ for the set of measurements in this study). For all of the T_g measurements presented below, transmission ellipsometry was performed using angles of incidence ranging from 45° to 58° . This range of angles provided a good ellipsometry signal within the constraints of the optical furnace. In the experiment, the ellipsometric angles P and A were measured as the sample temperature T was ramped up and down. Using the ellipsometric equations corresponding to an isotropic freely standing film and the measured P and A values at each measurement temperature, the temperature dependence of h and n was obtained [25]. The near-discontinuity in the expansivity $\alpha = (1/h)(\Delta h/\Delta T)$ at $T = T_g$ produces a ‘‘kink’’ in $h(T)$ and $n(T)$, which is also observed in both $P(T)$ and $A(T)$. It is the temperature at which this kink occurs that we identify as T_g . The determination of $h(T)$ from the ellipsometry data also allows the calculation of the expansivity in the glass and in the melt.

A technical difficulty associated with the measurement of freely standing PS films is the small contrast in the index of refraction between the PS film ($n = 1.59$ at room temperature) and the surrounding air. This results in small changes in P and A with temperature compared to those measured for the same film on a Si substrate for which the optical contrast is larger. As in all ellipsometric measurements, the relative sensitivity of the measurement decreases as the film thickness is decreased. Since T_g is obtained from the expansivity, which is a measure of the *relative* change in the film thickness, the T_g values for the thinnest films have the greatest relative error. For all of the measurements presented below, we obtained T_g values that were reproducible to within the experimental uncertainty of $\pm 2^\circ\text{C}$. We found that it was more difficult to achieve reproducible T_g values for the thinnest films ($h \sim 25$ nm) because of a reduced signal-to-noise ratio. For very thin freely standing films the alternative technique of Brillouin light scattering may be favored as the BLS

signal is independent of the film thickness, such that the sensitivity of the measurement does not decrease with decreasing film thickness [14,17–19,26].

Glass transition temperature measurements were performed upon both cooling and heating of the freely standing PS films, using temperature ramp rates of $|dT/dt| = 0.5^\circ\text{C}/\text{min}$ and $|dT/dt| = 1^\circ\text{C}/\text{min}$. There was no difference observed between the T_g values obtained using the two ramp rates; however, the slower ramp rate allowed more data points to be collected during a temperature ramp. The collection of more data points was especially important for the thinnest films to compensate for the lower signal-to-noise ratio. The faster ramp rate was used only for some of the measurements performed on films with $\bar{M}_w = 767 \times 10^3$ and $\bar{M}_w = 2240 \times 10^3$. All other measurements were performed using $|dT/dt| = 0.5^\circ\text{C}/\text{min}$.

After the preparation of the freely standing films, there are often small undulations or wrinkles in the film across the 4 mm diameter hole. Even if the film is very flat following preparation, wrinkles can form upon heating if there is a difference in the thermal expansion of the PS and the sample holder. The presence of the wrinkles produces a range of different angles of incidence for the light in the transmission ellipsometry experiment, which results in a broadening of the null in the light intensity measured at the detector. The large noise associated with such a broad null in the presence of wrinkles not only prohibits the measurement of T_g , it even prohibits the measurement of the film thickness at a given temperature. We avoid this problem by removing the wrinkles from the films using the following procedure. After the preparation of the freely standing films, the films are heated slowly to a temperature at which the wrinkles are observed to disappear with time. We find that the wrinkles are removed at temperatures that are close to the bulk value of T_g . After the wrinkles have been removed, as observed by the specular reflection of the laser light from the surface of the film, the measurement of the ellipsometric angles corresponding to a null in the light intensity is possible. In these measurements $P(T)$ and $A(T)$ are obtained not only on the first ramp down to a temperature less than T_g , but also on subsequent heating and cooling cycles. Typically T_g was measured for a given film on three or four successive heating and cooling temperature ramps. This allowed us to determine the effect of thermal cycling on the measured values of T_g .

After the T_g measurements were completed for each freely standing PS film, the film was transferred onto a Si substrate to allow an accurate absolute determination of the film thickness using reflection ellipsometry. The *absolute* film thickness values for the supported films were more accurate than those determined for the freely standing films because the uncertainty in the angle of incidence was much smaller ($\pm 0.005^\circ$) in the reflection ellipsometry experiment. In the transmission ellipsometry experiment, the angle of incidence was known only to about $\pm 0.5^\circ$ because of the use of a commercial rotation stage to mount the optical furnace. We note that, although the angle of incidence in the transmission ellipsometry experiment is known only to within $\pm 0.5^\circ$, the angle is fixed for a given measurement, such that

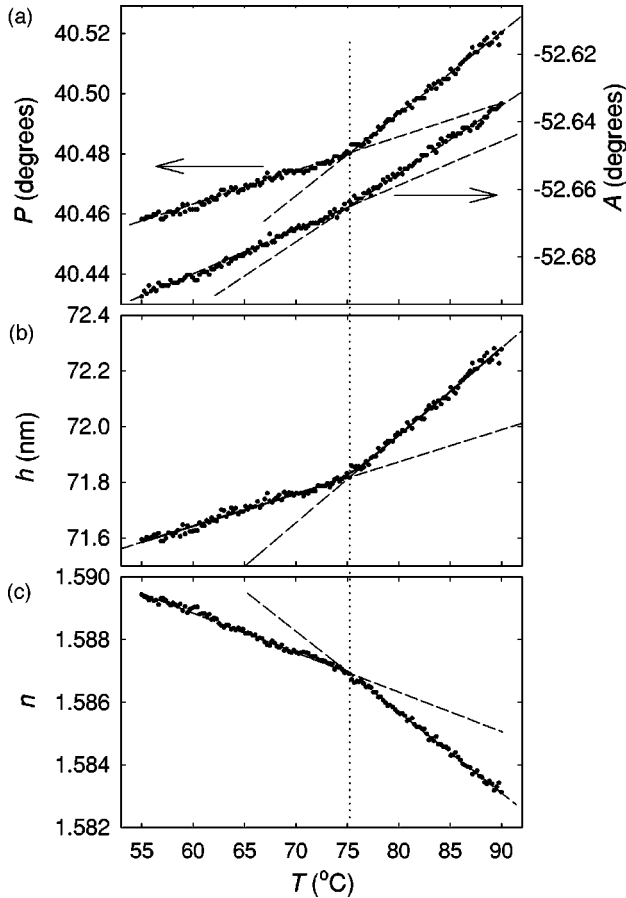


FIG. 1. (a) P and A data as a function of temperature for a freely standing PS film with $\bar{M}_w = 2240 \times 10^3$, $h = 71$ nm, and an angle of incidence of 58° . The data were obtained upon cooling the sample after several thermal cycles, as detailed in Table II. The dashed lines illustrate the linear regions of P and A in the glassy and melt regimes. (b) Plot of h obtained by fitting the data in (a). The solid line is the best fit of the data to Eq. (1), and the dashed lines illustrate the linear regions of h in the glassy and melt regimes. (c) Plot of n obtained from the data in (a). The dashed lines illustrate the linear regions of n in the glassy and melt regimes. The vertical dotted line indicates the average T_g value determined from the $h(T)$ and $n(T)$ data.

relative changes in the film thickness with temperature, and therefore T_g values, are measured very accurately.

RESULTS AND DISCUSSION

In Fig. 1(a) are shown representative transmission ellipsometry data obtained for a freely standing PS film with $\bar{M}_w = 2240 \times 10^3$ and $h = 71$ nm. The complete thermal history of this sample is given in Table II. Ellipsometry data were collected on each cooling and heating cycle. The data shown in Fig. 1(a) were collected during the cooling of the sample after two prior cooling and heating cycles of the freely standing film. By collecting data on many sequential cooling and heating cycles on the same sample, we were able to determine the effect of thermal cycling on the measured value of T_g . For every temperature cycle the T_g values agreed to within the experimental uncertainty of $\pm 2^\circ\text{C}$,

TABLE II. Thermal history of a PS film with $\bar{M}_w = 2240 \times 10^3$ and $h = 71$ nm.

Supported		
20 °C → 115 °C		(initial annealing)
115 °C → 20 °C		
Freely standing		
20 °C → 100 °C		(remove wrinkles)
100 °C → 55 °C		run 0 down ^a
55 °C → 90 °C		run 1 up
90 °C → 55 °C		run 1 down
55 °C → 90 °C		run 2 up
90 °C → 55 °C		run 2 down ^b
55 °C → 90 °C		run 3 up

^aStart data collection.

^bThis set of data is shown in Fig. 1(a).

with no systematic shift in the T_g values measured on the cooling and heating cycles. The reproducibility of the T_g measurement on different thermal cycles is illustrated in Fig. 2 for the sample described in Table II, and is typical of the results obtained for all samples. It is important to note that the T_g data for each freely standing PS film were obtained only after careful annealing of the film on the glass or mica substrate, as described above.

In Figs. 1(b) and 1(c) we plot the values of the film thickness $h(T)$ and index of refraction $n(T)$ obtained as discussed above. It is clear from Fig. 1 that the T_g value can be determined unambiguously since the measured ellipsometric angles $P(T)$ and $A(T)$ and the derived physical quantities $h(T)$ and $n(T)$ all display a kink at the same temperature, which we identify as T_g . The change in film thickness with temperature is, to within experimental uncertainty, linear for temperatures both lower and higher than T_g , as is expected on the basis of thermal expansion. Linear changes in n with

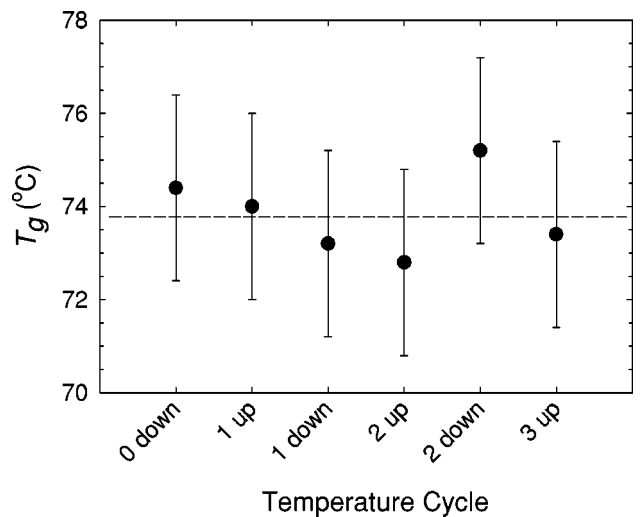


FIG. 2. T_g values obtained for a freely standing PS film with $\bar{M}_w = 2240 \times 10^3$, and $h = 71$ nm during the cooling and heating cycles described in Table II. The ellipsometry data for cycle “2 down” are shown in Fig. 1.

T are also observed for temperatures both lower and higher than T_g ; this is reasonable since the overall change of n with T is small (0.5%).

In the glass transition region the expansion coefficients vary from that of the glass to that of the melt. The transition between the expansion coefficients can be approximated by a tanh profile. From this it follows that quantities such as the film thickness, density, or refractive index should have a temperature dependence obtained simply by integrating the $\tanh(T)$ profile. This results in the following empirical expression which is valid for any measurement that varies linearly with temperature in the melt and glass region:

$$h(T) = w \left(\frac{M-G}{2} \right) \ln \left[\cosh \left(\frac{T-T_g}{w} \right) \right] + (T-T_g) \left(\frac{M+G}{2} \right) + c. \quad (1)$$

Here c is the value of the film thickness at $T=T_g$, w is the width of the transition between the melt and the glass, and M and G are the dh/dT slope values for the melt and glass, respectively. The value of T_g is obtained by fitting $h(T)$ to Eq. (1). This procedure is used to avoid the ambiguity associated with the standard determination of T_g by choosing the linear melt and glass portions of the data whose intersection defines T_g . Equation (1) has five parameters, while the standard way of determining T_g has four explicit parameters for the two linear regions; however there are an additional two implicit parameters in the choice made for the beginning and end of the transition region which are not included in the fit. The value of the width of the transition was kept constant so that the fit is not overdetermined and so that the nonlinear effect of the tanh profile on the expansion coefficient vanishes very rapidly with temperature above and below the transition region. Unfortunately, the scatter in the data and the small contrast between the melt and glass slopes does not allow us to determine the width of the transition other than to state that the transition is sharp (see Fig. 1) and that the choice of $w=2^\circ\text{C}$ resulted in excellent fits to the data in *all* cases. Larger values of the width, e.g., $w=5^\circ\text{C}$, resulted in notably worse fits to the data. The data for $n(T)$ were also fitted to Eq. (1) to obtain an independent value of T_g for each data set. The average of the T_g values obtained from $h(T)$ and $n(T)$ was used to obtain the T_g value for any given temperature ramp (see Fig. 2) and the average of the T_g values measured for multiple thermal cycles is the value quoted for each film. The difference between T_g values determined from $h(T)$ and $n(T)$ was always within experimental uncertainty.

There are two important aspects of the ellipsometry data and the fit of the ellipsometry data to Eq. (1) that distinguish our results for freely standing PS films from the recent results obtained by Kawana and Jones [15] on *supported* PS films. First of all, Kawana and Jones observe a broadening of the transition region between glass and melt with decreasing film thickness, with the midpoint of the transition shifting to lower temperatures. They claim that the decrease in T_g is a result of this broadening. In contrast, the transition that we observe for freely standing films is very sharp for all of our measurements (see Fig. 1, which is typical of all of the data).

A second significant difference between the ellipsometry results obtained for freely standing and supported PS films is the degree of linearity in the expansivities observed at temperatures that lie outside the transition region. For the supported films in [15], there is considerable deviation from linear expansivity, whereas our data for freely standing films are linear over a very broad temperature range. This difference may occur because the lateral constraint inherent to a film that is expanding or contracting on a substrate, in response to a change in temperature, does not apply to a freely standing film. Rather than being a contradiction, these two distinguishing features in the ellipsometry data reveal important fundamental differences between the glass transition in freely standing and in supported PS films.

For freely standing PS films on stainless steel sample holders, wrinkles form in the PS film upon heating because the expansivity of PS is much larger than that of the sample holder. As discussed above, the wrinkles are removed by annealing the samples at a temperature close to the bulk value of T_g , forming a smooth film across the 4 mm diameter hole on the sample holder. Upon subsequent cooling of the sample to measure T_g , an in-plane stress is produced in the PS film since the film contracts much more with decreasing temperature than does the stainless steel sample holder. The stress produced in the freely standing film depends on how much below T_g the sample is cooled in the T_g measurement. Typically it is necessary to cool 20°C to 30°C below T_g to obtain a sufficiently large data set in the glassy regime. In addition, the stress produced in the freely standing film depends on the mismatch in the thermal expansion coefficients of PS and the sample holder. We have evaluated the effect of the cooling-induced stress on the measured T_g values by using nylon sample holders instead of stainless steel sample holders to reduce the thermal expansion coefficient mismatch between the film and holder. The thermal expansion coefficients of glassy PS and nylon are the same to within experimental uncertainty [27], which reduces the cooling-induced stress dramatically relative to that obtained with the stainless steel sample holders, which have a thermal expansion coefficient that is smaller by a factor of ~ 5 . As a result of the expansivity mismatch, a sample cooled by 30°C on the stainless steel sample holder will have a lateral stress at least an order of magnitude larger than that for a sample on a nylon sample holder. For a given film thickness, we observed no difference between the T_g values measured for stainless steel and nylon sample holders, to within the uncertainty of the T_g measurement ($\pm 2^\circ\text{C}$). This result indicates that the small cooling-induced stress does not produce a substantial shift in the value of T_g .

We note that, although reproducible T_g values were obtained for different thermal cycles and different sample holder materials, the expansivities of the glass and melt were not reproducible. Qualitatively it was observed that the glass expansivity remained constant for all film thicknesses and that the melt expansivity decreased with decreasing film thickness. There is still no experimental consensus on this issue and the qualitative observation of this study is in agreement with the results in [13,14,16] and in disagreement with the results in [11,15].

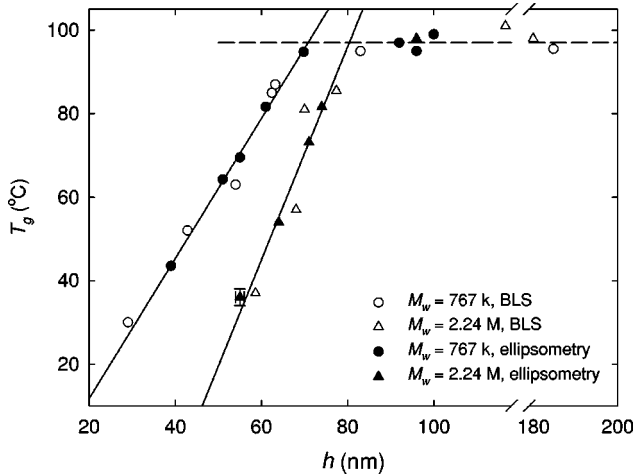


FIG. 3. Plot of T_g versus film thickness h for freely standing PS films with $\bar{M}_w = 767 \times 10^3$ and $\bar{M}_w = 2240 \times 10^3$. Two sets of data are shown: previous BLS data (open symbols) [6], and the transmission ellipsometry data obtained in the present study (solid symbols).

The ability to perform ellipsometry measurements on freely standing films at temperatures that are tens of degrees above T_g reveals important information about the dynamics of these samples. For freely standing PS films with $h > 100$ nm and molecular weights comparable to that used in the present study, many holes will form in the films in a relatively short time when they are held at a temperature that is only modestly greater than the bulk value of T_g [28]. For thinner PS films with a reduced value of T_g , hole formation is not observed until the film is heated to temperatures that are slightly below the bulk value of T_g [29]. This provides strong evidence that properties like viscosity, which are governed by the length scale of the entire chain and dominated by the slowest relaxation times, are qualitatively different from the dynamics occurring at smaller length scales which affect the glass transition.

In Fig. 3 are shown the T_g values obtained using BLS for freely standing PS films with two different molecular weight values [18], together with those obtained for freely standing PS films with the same two molecular weight values using transmission ellipsometry. The transmission ellipsometry data *quantitatively* agree with the previous BLS data [26]. All of the data can be described by the functional form

$$T_g = \begin{cases} T_g^b + \alpha(h - h_0), & h < h_0 \\ T_g^b, & h > h_0, \end{cases} \quad (2)$$

where T_g^b is the bulk value of T_g , h_0 is the threshold thickness value below which T_g reductions are observed, and α is the slope that describes the linear reduction of T_g with decreasing h for $h < h_0$. The fit to the data is specified by two parameters h_0 and α . Our analysis is *not* meant to imply that the h dependence of T_g is linear for h values less than the smallest values measured in the present study; however, within the h range that we measure, Eq. (2) provides an empirical description that is consistent with the data. Al-

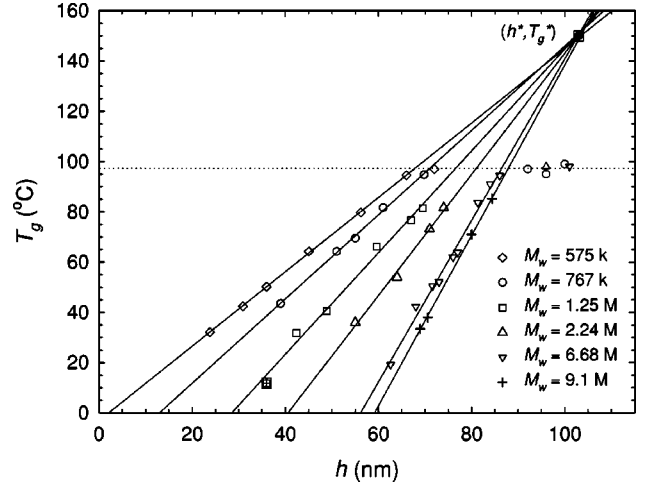


FIG. 4. Plot of T_g versus film thickness h for freely standing PS films for all of the molecular weights used in the present study ($575 \times 10^3 < \bar{M}_w < 9100 \times 10^3$). The straight solid lines are the best fits to the data in the regime in which T_g reductions are observed, and the horizontal dotted line corresponds to the bulk value of T_g .

though it is expected that $T_g(h)$ is smoothly varying near h_0 , the transition from one linear regime for $h > h_0$ to the other for $h < h_0$ is so abrupt that no significant deviation from the two linear regimes could be observed even though we invested considerable effort in the determination of T_g for h values close to h_0 . The surprisingly abrupt nature of the transition from reduced T_g values to bulk T_g values can be understood in terms of the existence of a mode of relaxation in the thin films that is distinct from bulk relaxation, as will be discussed below.

Molecular weight dependence

In Fig. 4 are shown all of the T_g values measured using transmission ellipsometry for freely standing PS films with different values of film thickness h and six different molecular weights, which differ by as much as a factor of ~ 15 (the root-mean-square end-to-end distance of the PS molecules R_{ee} ranges from 56 nm to 222 nm). This plot contains an extensive experimental quantification of the molecular weight dependence of T_g reductions for freely standing PS films in the limit of large \bar{M}_w . We find empirically that all of the data sets for each of the molecular weight values are described very well by Eq. (2). This means that each data set for a given molecular weight can be described by two best fit parameters: the threshold film thickness h_0 and the slope α that characterizes the linear decrease in T_g with decreasing film thickness. The lines calculated using the best fit values of h_0 and α for each molecular weight are also shown in Fig. 4.

From the calculated lines shown in Fig. 4, it can be seen that both h_0 and α increase monotonically with increasing \bar{M}_w . The simplest and most appealing explanation for the T_g reductions on the basis of chain confinement effects corresponds to reductions in T_g for film thicknesses less than the overall size of the PS molecules, e.g., R_{ee} , which scales as

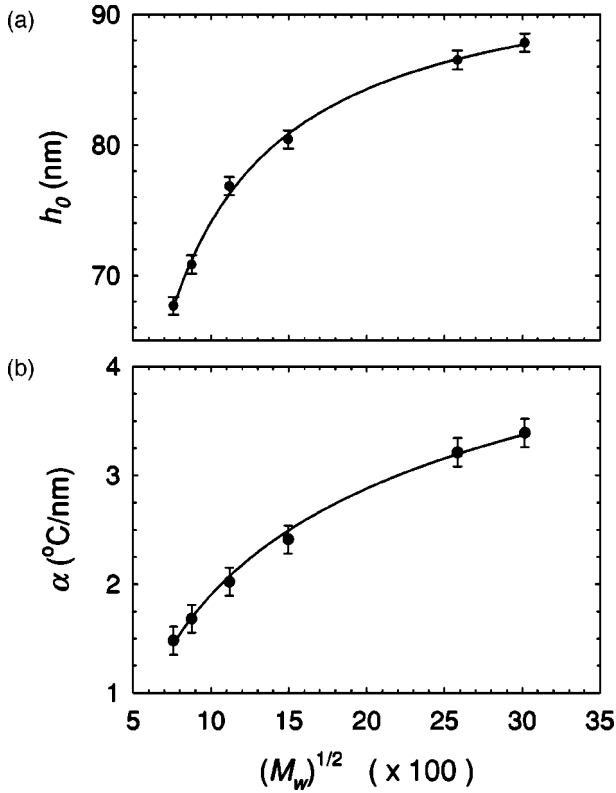


FIG. 5. (a) Plot of threshold thickness value h_0 versus the square root of the molecular weight. (b) Plot of slope α versus the square root of the molecular weight. For both plots, the solid line is a curve meant to guide the eye.

$\bar{M}_w^{1/2}$. This implies that h_0 should scale as $\bar{M}_w^{1/2}$. In Fig. 5 we show the dependence of the best fit values of both h_0 and α on $\bar{M}_w^{1/2}$, with error bars obtained from the least squares fits of the data in Fig. 4 to Eq. (2). The simple scaling behavior of $h_0 \sim \bar{M}_w^{1/2}$ is *not* observed. To facilitate comparison of the present experimental results with those of future theoretical models, we provide the α and h_0 best fit values in Table I.

Scaling analysis

We continue now with the discussion of a rather surprising aspect of the data revealed by extrapolating the best fit straight lines to larger values of T_g and h . The extrapolation suggests a common intersection point (h^*, T_g^*) of all of the best fit lines to the data obtained for $T_g < T_g^b$. From the data shown in Fig. 4, the intersection point is specified by $h^* = (103 \pm 1)$ nm and $T_g^* = (150 \pm 2)$ °C. In a system in which there are two competing mechanisms for mobility, the faster, more efficient mode will dominate the behavior. The presence of a mode of mobility (distinct from the cooperative motion near T_g in bulk samples) that dominates in very thin films can explain the sharp transition between the bulk T_g values measured for the thickest films and the reduced T_g values measured for the thinnest films. Although we do not imply any significance to measured T_g data in the extrapolated regime of the fits, this surprising result does strongly suggest that the point (h^*, T_g^*) is important to the under-

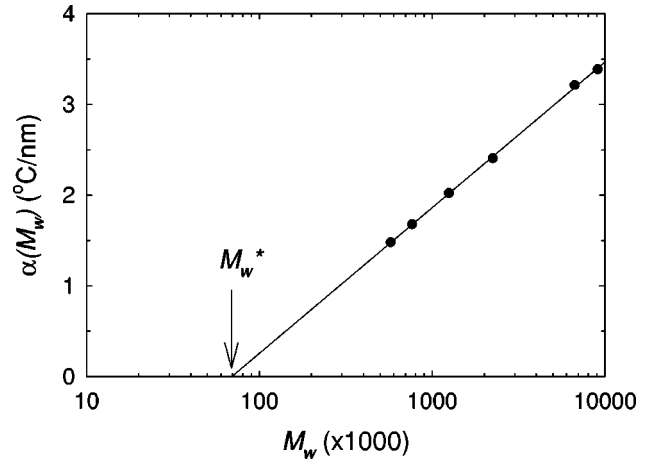


FIG. 6. Plot of the slope $\alpha(\bar{M}_w)$ characterizing the linear depression in T_g with h versus \bar{M}_w .

standing of a second mechanism for mobility which dominates for thin films ($h \lesssim R_{ee}$). The existence of a common intersection point for all of the extrapolated best fit curves in Fig. 4 shows that $(T_g - T_g^*) \propto (h - h^*)$. Clearly, all of the data can be parametrized if we define a \bar{M}_w -dependent parameter $\alpha(\bar{M}_w)$, which represents the slope of the linear reduction in T_g with decreasing h for a given \bar{M}_w :

$$(T_g - T_g^*) = \alpha(\bar{M}_w)(h - h^*). \quad (3)$$

Given Eq. (3), an understanding of the origin of $\alpha(\bar{M}_w)$ becomes crucial to the understanding of the \bar{M}_w dependence of the anomalous T_g results for thin freely standing films. To gain some insight into the possible dependencies of $\alpha(\bar{M}_w)$, we plot $\alpha(\bar{M}_w)$ in Fig. 6. The data fit remarkably well to a straight line on the semilogarithmic plot, but any functional form that parametrizes the slope of the T_g reduction with decreasing h to molecular weight can be used equally well in the subsequent analysis. Following the suggestion from the data in Fig. 6, we obtain the expression

$$\alpha(\bar{M}_w) = b \ln(\bar{M}_w / \bar{M}_w^*), \quad (4)$$

where $b = (0.70 \pm 0.02)$ °C/nm and $\bar{M}_w^* = (69\,000 \pm 4000)$. While the parametrization given by Eq. (4) is only strictly valid for \bar{M}_w within the range studied, we note that extrapolating to \bar{M}_w^* leads to $\alpha(\bar{M}_w) = 0$. The implication is that for polymers with $\bar{M}_w < \bar{M}_w^*$ no chain confinement effects due to this second mode can possibly be observed. Perhaps more importantly for comparison to the data, we can use Fig. 4 to show that for $\alpha(\bar{M}_w) = (T_g^* - T_g^b)/h^* \sim 0.5$ °C/nm no T_g reductions will be observed for any film with nonzero thickness. From Fig. 6 it is evident that this value of $\alpha(\bar{M}_w)$ corresponds to a $\bar{M}_w \sim 150 \times 10^3$.

An extensive study of T_g for low \bar{M}_w found that for $\bar{M}_w < 380 \times 10^3$ the T_g reductions were independent of \bar{M}_w and reductions in T_g were observed for $h < 50$ nm [19,14]. (We

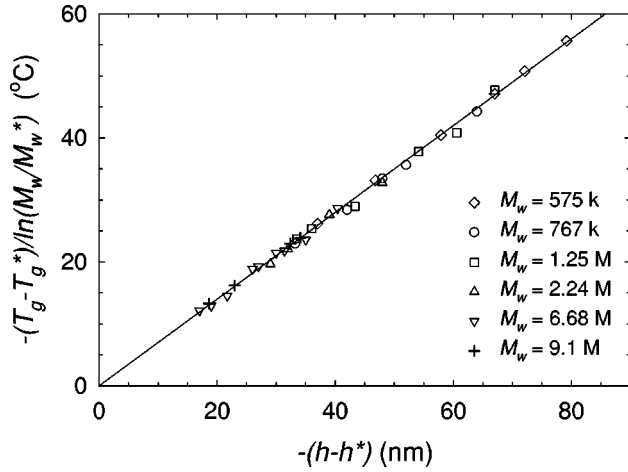


FIG. 7. Scaling of all of the reduced T_g values for all molecular weights and film thicknesses studied as described by Eq. (5).

note that where the \bar{M}_w of the two studies overlap quantitative agreement of the T_g values was obtained.) In contrast to any mechanism responsible for reductions of T_g resulting from confinement effects, the reduced T_g values for low \bar{M}_w values have been attributed to a finite size effect due to an intrinsic length scale for cooperative dynamics [19]. Clearly, for some range of values of \bar{M}_w these finite size effects must compete directly with the chain confinement effects. To examine the regime corresponding to the crossover between the domination of each effect, we consider the following. Since T_g reductions due to the intrinsic length scale of glass transition dynamics are observed to occur for $h \sim 50$ nm, we consider the straight line between (h^*, T_g^*) and the point $(h = 50 \text{ nm}, T_g^b)$ in Fig. 4. From the slope of this line, $\alpha \sim 1$ °C/nm, and Fig. 6, we can see that only modest T_g reductions due to chain confinement effects in thin films should be observed for $\bar{M}_w \sim 300 \times 10^3$. Since the T_g reductions due to the finite size effects discussed in [14,19] are larger than the mechanism important for chain confinement effects, this value of \bar{M}_w is a lower limit for a crossover between the two mechanisms. This value for the crossover \bar{M}_w is in excellent agreement with that measured experimentally [14,19].

To summarize, from the experimental data we obtain Eqs. (3) and (4). Equation (3) suggests a mode of mobility different from that observed in the bulk and hence has important theoretical implications. Equation (4) is merely a satisfactory empirical parametrization convenient for quantifying the relationship between T_g and h . A detailed understanding of the data requires a theoretical argument for an acceptable form of $\alpha(\bar{M}_w)$. Combining Eqs. (3) and (4), we obtain a single relationship expressing the glass transition temperature in terms of film thickness and molecular weight:

$$(T_g - T_g^*) = b \ln(\bar{M}_w / \bar{M}_w^*) (h - h^*). \quad (5)$$

In Fig. 7 we test the scaling expression of Eq. (5) explicitly. Figure 7 contains all the reduced T_g data for all the molecu-

lar weights in the high \bar{M}_w regime ($> 350 \times 10^3$), and we find that the data are quantitatively described by only four parameters: T_g^* , h^* , \bar{M}_w^* , and b . We expect that these four parameters will describe the T_g reductions observed for all PS samples with $575 \times 10^3 < \bar{M}_w < 9100 \times 10^3$.

General issues related to the T_g for high \bar{M}_w PS

There are several concerns associated with the preparation and treatment of high \bar{M}_w PS films. One concern with the use of the very high \bar{M}_w polymers in the present study is the possibility of chain scission occurring during the spin-coating deposition of the films. The likelihood of chain scission is expected to increase with increasing \bar{M}_w , and it would result in a shift in the average \bar{M}_w to smaller values and a considerable broadening of the \bar{M}_w distribution. This broadening of the \bar{M}_w distribution is expected to produce a broadening of the transition region between the glass and melt regimes. For example, if we consider PS molecules of the highest \bar{M}_w value, $\bar{M}_w = 9100 \times 10^3$, chain scission would result in a considerable number of molecules with, on average, half of the original \bar{M}_w value. As a specific example, consider a film with $h = 70$ nm, $\bar{M}_w = 9100 \times 10^3$, for which $T_g = 37$ °C. Chain scission would result in a continuous, broad distribution of \bar{M}_w values, with a significant fraction of molecules with, e.g., $\bar{M}_w = 2240 \times 10^3$ and $\bar{M}_w = 6680 \times 10^3$. Because the T_g values for $h = 70$ nm films with $\bar{M}_w = 2240 \times 10^3$ and $\bar{M}_w = 6680 \times 10^3$ are 71 °C and 44 °C, respectively, the glass transition should be broadened by as much as 25 °C. Since there is no evidence for a broadening of the transition region even for films with the largest values of \bar{M}_w , we conclude that chain scission does not occur to any appreciable extent during the spin-coating procedure.

Another concern associated with the sample preparation is related to the annealing history of the PS films on the glass or mica substrates. Ideally, the samples must be annealed to establish an equilibrium chain conformation. Attaining equilibrium chain conformations is expected to require annealing times on the order of the reptation (or terminal) time τ_r , which we will demonstrate is not feasible for very high \bar{M}_w . Measurements of the creep compliance of PS with $\bar{M}_w = 385 \times 10^3$ reveal that the end of the ‘‘plateau’’ region corresponding to the reptation time occurs at $\tau_r \sim 3 \times 10^3$ s at a temperature of 115 °C [30] (the annealing temperature of the samples in the present study). Since $\tau_r \sim \bar{M}_w^{3.4}$ we can obtain τ_r for the various \bar{M}_w values of this study to establish annealing times t . For the two lowest \bar{M}_w values, 575×10^3 and 767×10^3 , the relaxation times are $\tau_r \sim 3$ h and $\tau_r \sim 9$ h, such that the annealing time $t (= 12 \text{ h}) > \tau_r$. This analysis indicates that these samples are suitably annealed. However, for the higher molecular weights used in the present study $t \ll \tau_r$ due to the strong \bar{M}_w dependence of τ_r . Specifically, for the highest \bar{M}_w value, $\tau_r \sim 4.5$ years, which is a time scale that is not easily accessible to experiment. Simply raising the annealing temperature is also not feasible since holes

will form in the thin films. Hole formation *is* an indication of flow in the polymer melt, but this should *not* be taken as an indication that τ_r is comparable to the experimental time scale. In the initial stages of hole formation, a hole forms as a result of the dispersion force acting on the interfaces; after the hole forms, it grows as a result of surface tension. In both stages the flow of polymers is *driven*, which can result in alignment of the chains and “shear thinning” with dynamics that are much faster than τ_r . For example, a PS film with $h = 100$ nm, $\bar{M}_w = 767 \times 10^3$, and at a temperature of 115°C will have a reduction in the viscosity of at least an order of magnitude as a result of nonlinear viscoelastic effects (shear thinning) [28]. Proper annealing of the highest \bar{M}_w film would require raising the temperature to 160°C for 12 h which can result in dewetting of the film.

Given that it is not feasible to anneal the samples for $t > \tau_r$ it is important to determine the effect of this on the measured value of T_g . We proceed by discussing several reasons why the annealing times used in this study are sufficient for the purposes of a T_g measurement.

The glass transition in the bulk is dependent on segmental mobility in the PS chains. We consider the polymer chain of length N as made up of a series of subchains between entanglement points of length N_e . For the PS molecules used in the present study, $N \gg N_e$. We can compare the characteristic time τ_{N_e} associated with the longest Rouse modes of the subchain with the annealing time t . Annealing for times longer than τ_{N_e} would mean that any nonequilibrium features as large as $\sim R_{ee} \sqrt{N/N_e}$ are relaxed and equilibrium configurations at the length scale of N_e are easily reached. For example, nonequilibrium density fluctuations can be relaxed without a reordering of the entanglement network. For this case relaxation of the subchains of length $\sim N_e$ combined with the associated expansion or compression of the entanglement network is all that is required. Supporting evidence for this point is provided by the experimental observation that, while the reptation time in the bulk is strongly dependent on \bar{M}_w , the glass transition is not (measurements of shear storage modulus for different \bar{M}_w values reveal this point very clearly [30]). Studies of creep compliance show that for PS at 115°C , this criterion corresponds to a time $\tau_{N_e} \sim 100$ s [30], which is much smaller than t . Therefore, since all of the chains are annealed for times $t \gg \tau_{N_e}$, sufficient annealing for the usual glass transition (dependent on segmental mobility) has been achieved. While perturbations like density fluctuations are relaxed easily, any anomaly in the glass transition *dependent on \bar{M}_w* , and hence chain confinement effects, may still be influenced by annealing times $\tau_{N_e} < t < \tau_r$, and this point is discussed below.

Any chain confinement effect has to depend on deviations from the bulk intrinsic equilibrium conformation of the chains and we have to consider the effect of anisotropy in chain conformations due to spin coating or any other nonequilibrium process in the preparation of the samples. The anisotropy induced in the chain conformations by sample preparation could not have the strong film thickness dependence, and in particular the sudden onset for $h = h_0$, that is

observed in our T_g measurements. For instance, in the spin-coating process, a chain would be stretched in the radial direction as a result of the forces acting on it while spinning. However, this effect will occur in all films *regardless of the film thickness*, and if there was a correlation between chain anisotropy due to nonequilibrium processes and the T_g value, a film with thickness $h > h_0$ should exhibit the *same reductions* in T_g as a film with $h < h_0$. As this is not observed, the insufficient annealing of nonequilibrium conformations due to sample preparation is unlikely to make a significant contribution to the observed T_g reductions. There are two more reasons why the annealing history of the samples is sufficient for a reliable measure of T_g as evidenced by the data. The \bar{M}_w dependence of the slope parameter α , shown in Fig. 6, is uniform and well described by Eq. (4) for the entire range of \bar{M}_w values and in particular does not show any difference in behavior between chains that are annealed for $t > \tau_r$ ($\bar{M}_w = 575 \times 10^3, 767 \times 10^3$) and chains for which $t < \tau_r$ ($\bar{M}_w = 1250 \times 10^3$ up to 9100×10^3). Lastly, the dependence of α on \bar{M}_w becomes weaker with increasing \bar{M}_w (see Figs. 4 and 5). This dependence is inconsistent with the interpretation that the annealing history is responsible for the observed data since the films with $t \ll \tau_r$ have configurations that are farthest from equilibrium, and should thus show the largest anomalies in T_g .

We conclude our discussion of the experimental results and analysis with an appealing theoretical idea that has recently been proposed by de Gennes as a potential explanation of the data shown in Fig. 4 [31]. The abrupt change from the bulk T_g value to reduced T_g values as h is decreased is highly suggestive of the existence of another type of chain motion that is unimportant in bulk samples, but becomes more efficient for thin films. De Gennes has suggested the possibility of an additional mode of mobility where the chain moves (or slides) in the direction of the primitive path. This “sliding” motion becomes important in films thinner than R_{ee} because of the existence of chain segments at one interface forming loops and chain segments spanning the film forming bridges. In the model it is suggested that the loops and bridges, coupled with a high mobility at the polymer free surfaces, provide extra mobility within the film, thereby reducing T_g . This tentative model proposes a competition between the usual α relaxation processes related to the bulk glass transition and the relaxation associated with the sliding motion [31], and results in a linear reduction of T_g with decreasing film thickness in qualitative agreement with the data presented here.

CONCLUSIONS

We present the results of an extensive experimental investigation of the molecular weight dependence of T_g in thin freely standing polymer films with six different large molecular weight values ranging from 575×10^3 to 9100×10^3 . The \bar{M}_w dependence of the T_g reductions for the large \bar{M}_w regime demonstrates that chain confinement effects are important to understand the observed behavior. This behavior is distinct from that in the low \bar{M}_w regime, which is dominated

by finite size effects [14,19]. We observe sharp transitions for all films, with different values of \bar{M}_w and film thickness h , with a linear reduction in T_g for h less than a threshold film thickness value. While the results of the present study do not allow the unique identification of the mechanism responsible for the T_g reductions, the reliable and reproducible nature of the data is able to test existing and new theories of the effect of chain confinement on the glass transition in thin polymer films. The abrupt transition from the bulk T_g value to reduced T_g values with decreasing h is suggestive of two competing modes of motion acting in the two distinct re-

gimes. The \bar{M}_w dependence of the T_g values suggests that one of the modes is related to confinement of the polymer chain. We have shown how a simple scaling analysis describes all T_g values measured for freely standing PS films with $575 \times 10^3 < \bar{M}_w < 9100 \times 10^3$.

ACKNOWLEDGMENTS

We thank Professor P.-G. de Gennes and Professor G. B. McKenna for insightful discussions. Financial support from NSERC of Canada is gratefully acknowledged.

-
- [1] M.H. Cohen and G.S. Grest, *Phys. Rev. B* **20**, 1077 (1979).
 [2] See, for example, the collections of papers in *J. Res. Natl. Inst. Stand. Technol.* **102**, 135 (1997), *J. Non-Cryst. Solids* **235-237**, 1 (1998), and *J. Phys.: Condens. Matter* **11**, A1 (1999).
 [3] W. Götze and L. Sjögren, *Rep. Prog. Phys.* **55**, 241 (1992).
 [4] G. Adam and J.H. Gibbs, *J. Chem. Phys.* **43**, 139 (1965).
 [5] C. Bennemann, C. Donati, J. Baschnagel, and S. Glotzer, *Nature (London)* **399**, 246 (1999).
 [6] C.L. Jackson and G.B. McKenna, *Chem. Mater.* **8**, 2128 (1996).
 [7] M. Arndt, R. Stannarius, H. Groothues, E. Hempel, and F. Kremer, *Phys. Rev. Lett.* **79**, 2077 (1997).
 [8] S.H. Anastasiadis *et al.*, *Phys. Rev. Lett.* **84**, 915 (2000).
 [9] A.K. Rizos and K.L. Ngai, *Phys. Rev. E* **59**, 612 (1999).
 [10] J.A. Forrest and R.A.L. Jones, in *Polymer Surfaces, Interfaces and Thin Films*, edited by A. Karim and S. Kumar (World Scientific, Singapore, 2000).
 [11] J.L. Keddie, R.A.L. Jones, and R.A. Cory, *Europhys. Lett.* **27**, 59 (1994).
 [12] J.L. Keddie, R.A.L. Jones, and R.A. Cory, *Faraday Discuss.* **98**, 219 (1994).
 [13] W. Wallace, J.H. van Zanten, and W. Wu, *Phys. Rev. E* **52**, R3329 (1995).
 [14] J. Mattson, J.A. Forrest, and L. Börjesson, *Phys. Rev. E* **62**, 5187 (2000).
 [15] S. Kawana and R.A.L. Jones (unpublished).
 [16] G.B. DeMaggio, W.E. Frieze, D.W. Gidley, M. Zhu, H.A. Hristov, and A.F. Yee, *Phys. Rev. Lett.* **78**, 1524 (1997).
 [17] J.A. Forrest, K. Dalnoki-Veress, J.R. Stevens, and J.R. Dutcher, *Phys. Rev. Lett.* **77**, 2002 (1996); **77**, 4108 (1996).
 [18] J.A. Forrest, K. Dalnoki-Veress, and J.R. Dutcher, *Phys. Rev. E* **56**, 5705 (1997).
 [19] J.A. Forrest and J. Mattson, *Phys. Rev. E* **61**, R53 (2000).
 [20] J.A. Forrest, C. Svanberg, K. Revesz, M. Rodahl, L.M. Torell, and B. Kasemo, *Phys. Rev. E* **58**, R1226 (1998).
 [21] The authors of Ref. [13] *infer* a T_g value higher than their highest measurement temperature for a thin PS film because T_g is not measured within the experimental temperature window. Their result can also be interpreted as an inability to resolve T_g due to the decreasing contrast between the melt and glass slopes observed by others as well as in Ref. [13] as the film thickness is reduced.
 [22] Y. Grohens, M. Brogly, C. Labbe, M.O. David, and J. Schultz, *Langmuir* **14**, 2929 (1998).
 [23] R.L. Jones, S.K. Kumar, D.L. Lo, R.M. Briber, and T.P. Russell, *Nature (London)* **400**, 146 (1999).
 [24] J.A. Forrest and K. Dalnoki-Veress, *Adv. Colloid Interface Sci.* (to be published).
 [25] R.M.A. Azzam and N.M. Bashara, *Ellipsometry and Polarized Light* (North-Holland Publishing Company, Amsterdam, 1977).
 [26] J.R. Dutcher, K. Dalnoki-Veress, and J.A. Forrest, in *Supramolecular Structures in Confined Geometries*, edited by S. Manne and G.G. Warr, ACS Symposium Series No. 736 (American Chemical Society, Washington, DC, 1999).
 [27] *Polymer Handbook*, 3rd ed., edited by J. Brandrup and E.H. Immergut (Wiley, New York, 1989).
 [28] K. Dalnoki-Veress, B.G. Nickel, C.B. Roth, and J.R. Dutcher, *Phys. Rev. E* **59**, 2153 (1999).
 [29] C.B. Roth, K. Dalnoki-Veress, B.G. Nickel, and J.R. Dutcher (unpublished).
 [30] G. Strobl, *The Physics of Polymers*, 2nd ed. (Springer-Verlag, Berlin, 1997).
 [31] P.-G. de Gennes, *Eur. Phys. J. E* **2**, 201 (2000).